

# Experimental Correlation between Anomalous Electron Collision Frequency and Plasma Turbulence in a Hall Effect Thruster

IEPC-2019-843

*Presented at the 36th International Electric Propulsion Conference  
University of Vienna, Austria  
September 15-20, 2019*

Zachariah A. Brown\*, Ethan Dale† and Benjamin A. Jorns‡  
*University of Michigan, Ann Arbor, Michigan, 48105, United States of America*

The anomalous electron transport in a magnetically shielded Hall thruster is experimentally investigated. Direct measurements of anomalous collision frequency from LIF measurements are compared to predicted values using quasi-linear for the electron drift instability and measurements of plasma wave turbulence. Throughout the near-field region the two values agree to within an order of magnitude and share similar spatial trends, but quasi-linear consistently over predicts the collision frequency within the acceleration region. These results may be indicative of non-Maxwellian electrons or non-linear effects in the near-field plume.

## I. Introduction

The Hall thruster is a cylindrical crossed-field plasma device commonly used for in-space propulsion. These devices produce thrust by accelerating ions across an applied axial electric field between an anode, where gas is injected, and a downstream cathode. The propellant is ionized by electrons emitted from the cathode and to increase residence time and ionization efficiency a radial magnetic field is applied that impedes electron mobility, but is insufficient to magnetize the ions. The crossed magnetic and electric fields results in a high speed azimuthal  $E \times B$  drift. Due to the high speed electrons, as well as possible field and density gradients, Hall thrusters are subject to a plethora of plasma instabilities that can govern the overall operation and performance of the devices.<sup>1</sup> While the presence of these instabilities have not prevented Hall thruster operation and deployment, they pose a major impediment to the development of Hall thruster simulations and predictive modeling.

Hall thruster simulations often rely on 2D (r-z) axisymmetric grids where the ion motion is governed by particle-based methods and, due to computational limitations, the electrons are treated as a fluid. The electron mobility is therefore governed by Ohm's Law. Numerous works have shown that solely using particle collision based resistivity does not properly resolve Hall thruster properties. An anomalous resistivity term must be added to account for kinetic processes that cannot be captured by the electron fluid model. This anomalous term can be determined either from experimental data or predicted using theory.<sup>2</sup> While many theories<sup>3-8</sup> have been proposed to determine this anomalous term there is currently no definitive answer.

In recent years a growing consensus has emerged pointing towards the electron drift instability (EDI) as the dominant contributor to anomalous electron mobility. Fully kinetic codes, either 1D in the azimuthal direction or 2D (r- $\theta$ ), have suggested the presence of this instability in Hall thrusters<sup>9-16</sup> and analytical models have been developed that demonstrate the instability's impact on mobility.<sup>17-19</sup> In spite of the substantial and promising numerical results there has been limited experimental verification of both the instability's existence and effect. While collective Thomson scattering and electrostatic probes have both

---

\*PhD Candidate, Aerospace Engineering, brownzac@umich.edu.

†PhD Candidate, Aerospace Engineering, etdale@umich.edu.

‡Assistant Professor, Aerospace Engineering, bjorns@umich.edu .

measured oscillations in the Hall plume bearing resemblance to the EDI there has be no direct comparison between an experimentally measured anomalous collision frequency and the values predicted by theory and wave measurements that would demonstrate the impact of the EDI.<sup>20-22</sup> There is an apparent need to resolve this uncertainly of EDI's contribution to anomalous mobility using experimental methods.

The goal of this work is to address if the mobility profile observed in Hall thrusters is directly related to the onset of the EDI based on current theory. This paper is organized in the following way, in Section II. we present a framework for evaluating anomalous collision frequency based on Hall thruster plume properties and plasma wave turbulence. Then in Section III. we review current models of the EDI and present the quasi-linear theory used for evaluating its contribution to anomalous mobility. In Section IV. we describe the experimental methods used to both measure the anomalous collision frequency and EDI wave properties. In Section V. we present and compare the measured and theoretical profiles and finally in Section VI. we draw conclusions about the impact of the EDI on thruster dynamics and the implications for numerical modeling.

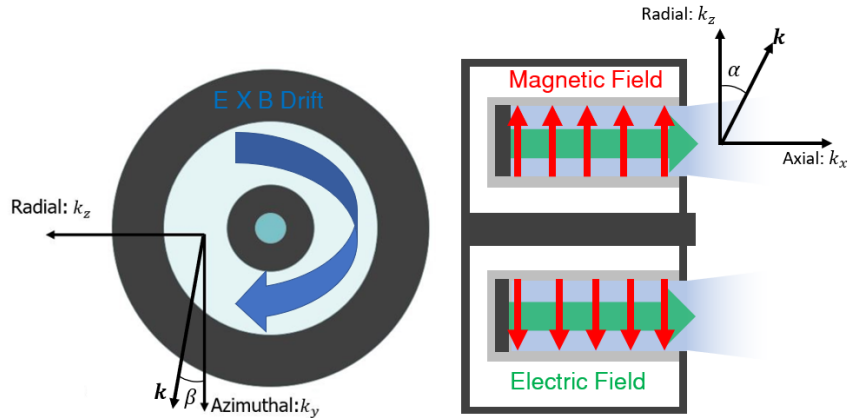


Figure 1: Schematic of a Hall thruster with the wave direction coordinate system. The components are  $k_x$  along the electric field vector,  $k_y$  in the  $E \times B$  direction, and  $k_z$  along the magnetic field lines.

## II. Turbulence Driven Transport

In section we develop a framework for both predication of anomalous collision frequency from theory and calculation from experimental data. We start with the momentum conservation equation for elections,

$$\frac{\partial}{\partial t}(mn_e \vec{V}_{de}) + \nabla \cdot (mn_e \vec{V}_{de} \vec{V}_{de}) = qn_e(\vec{E} + \vec{V}_{de} \times \vec{B}) - \nabla \cdot \bar{\Pi} - mn_e \nu_c \vec{V}_{de} \quad (1)$$

Here  $m_e$ ,  $n_e$ ,  $\vec{V}_{de}$ , and  $\bar{\Pi}$  are the electron mass, number density, drift velocity, and pressure tensor respectively,  $\vec{E}$  and  $\vec{B}$  are the local electric and magnetic fields, and  $\nu_c$  is the classical electron-neutral collision frequency. We further assume the magnetic field is purely radial in the “z” direction and the electron inertial and pressure terms are negligible to produce a set of equations for the axial(“x”) and azimuthal(“y”) directions(see Fig.1):

$$0 = qn_e E_x - qn_e V_{dey} B_z - mn_e \nu_c V_{dex}, \quad (2)$$

$$0 = qn_e E_y + qn_e V_{dex} B_z - mn_e \nu_c V_{dey}. \quad (3)$$

Following the techniques of Davidson and Krall,<sup>23</sup> we take the time average, on the time scale of the anticipated plasma instabilities, and note that  $\langle n_e E_y \rangle$  will be non-zero if density and electric field perturbations have components that are in phase. With some algebra, we combine Eqn.2 and 3 to solve for the effective axial electron mobility ( $\mu_{eff} \equiv v_{Dex}/E_x$ ):

$$\mu_{eff} = \frac{\mu_c}{1 + \Omega^2} \left( 1 - \Omega \frac{\langle n_e E_y \rangle}{n_e E_x} \right). \quad (4)$$

Where  $\mu_c = e/m_e\nu_c$  is the classical mobility coefficient and  $\Omega$ , the so-called Hall parameter, is the ratio of the electron cyclotron frequency and the classical collision frequency ( $\omega_{ce}/\nu_c$ ). Here we see that if the instability correlation term ( $\langle n_e E_y \rangle$ ) is non-zero and negative the effective mobility will increase while in the absence of oscillations the mobility reduces to the classical result across magnetic fields. In the limit of large Hall parameter ( $\Omega \gg 1$ ), commonly met in Hall thruster plumes, the mobility equation simplifies to:

$$\mu_{eff} = \frac{1}{B_z \omega_{ce}} \left( \nu_c - \omega_{ce} \frac{\langle n_e E_y \rangle}{n_e E_x} \right) = \frac{\nu_{eff}}{B_z \omega_{ce}}, \quad (5)$$

where we have defined an effective collision frequency  $\nu_{eff} = \nu_c - \omega_{ce} \langle n_e E_y \rangle / n_e E_x$ . The second term in this definition is often denoted as an anomalous collision frequency ( $\nu_{AN}$ ). For modelers using a fluid-code for electrons this anomalous collision is either based on experimental data or invoke a closure equation informed from kinetic simulations. The following section will introduce the quasi-linear theory used to calculate  $\langle n_e E_y \rangle$  for the electron drift instability.

### III. Electron Drift Instability

The  $E \times B$  drift of electrons serve as a potential energy source for instability growth. In 2004, 2D particle-in-cell simulations first showed the presence of strong azimuthal oscillations that develop on the millimeter scale and oscillate on the order of Mhz in a Hall thruster plume.<sup>24</sup> Following the analytical work of Ducrocq, Cavalier, and et al.,<sup>17,18</sup> the dispersion relation of the EDI in a Hall thruster geometry is given by

$$1 + k^2 \lambda_{De}^2 + g \left( \frac{\omega - k_y V_{De y}}{\omega_{ce}}, (k_x^2 + k_y^2) \rho^2, k_z^2 \rho^2 \right) - \frac{k^2 \lambda_{De}^2 \omega_{pi}^2}{(\omega - k_x V_p)} = 0, \quad (6)$$

where  $g(\Omega, X, Y)$  is the Gordeev function defined as

$$g(\Omega, X, Y) = i\Omega \int_0^{+\infty} e^{-X[1-\cos(\varphi)] - \frac{1}{2}\varphi^2 + i\Omega\varphi} d\varphi. \quad (7)$$

Here  $\omega$  is the oscillation frequency,  $\omega_{ce}$  is the electron cyclotron frequency,  $\omega_{pi}$  is the ion plasma frequency,  $k = \sqrt{k_x^2 + k_y^2 + k_z^2}$  is the oscillation wavenumber,  $k_x$  is the wavevector component traveling in the axial direction,  $k_y$  is the component in the  $E \times B$  direction,  $k_z$  is the component in the radial direction (along magnetic field lines),  $V_{De y}$  is the azimuthal electron drift velocity,  $V_p$  is the ion beam velocity in the axial direction,  $\lambda_{De}$  is the Debye length, and  $\rho = V_{the}/\omega_{ce}$  is the electron Larmor radius at thermal velocity  $V_{the} = \sqrt{qT_e/m}$  where  $T_e$  is expressed in electron-volts.

In order to relate this instability to the anomalous collision frequency we must use this dispersion to calculate the  $\langle n_e E_y \rangle$  term in Eqn.5. First, we represent the perturbations of density and electric we as propagating waves with a Fourier decomposition of

$$\begin{aligned} \delta n_e &= \sum_{k_y} n_{e(k_y)} e^{i(k_y y - \omega t)} + \text{c.c.} \\ \delta E_y &= -i \sum_{k_y} k \phi_{(k_y)} e^{i(k_y y - \omega t)} + \text{c.c.} \end{aligned} \quad (8)$$

where c.c. denotes complex conjugate, and  $n_{e(k_y)}$  and  $\phi_{(k_y)}$  are the Fourier amplitudes of the density and potential oscillations. We have also employed the electrostatic approximation  $\delta \vec{E} = -\nabla \phi_{(\vec{k})} = -ik_y \phi_{(k_y)}$  where  $\phi_{(k_y)}$  are fluctuations in plasma potential. With these relations the anomalous collision frequency is given by

$$\nu_{AN} = \omega_{ce} \frac{\langle \delta n_e \delta E_y \rangle}{n_e E_x} = \frac{\omega_{ce}}{E_x} \text{Im} \left[ \sum_{k_y} k_y \frac{n_{e(k_y)}}{n_{e0}} \phi_{(k_y)} \right], \quad (9)$$

where  $n_{e0}$  is the unperturbed electron density. The potential fluctuations  $\phi_{(k_y)}$  are correlated by:<sup>17,18</sup>

$$n_{e(k_y)} = \frac{en_{e0}}{mV_{the}^2} \phi_{(k_y)} (1 + g(\Omega, X, Y)) \quad (10)$$

where  $g(\Omega, X, Y)$  is the Gordeev function from in Eqn. 7. Combining Eqns.9 and 10 yields a general expression for anomalous collision due the EDI:

$$\nu_{AN} = -\frac{\omega_{ce}}{E_x} T_e \text{Im} \left[ \sum_{k_y} \left( \frac{\phi(k_y)}{T_e} \right)^2 k_y g \left( \frac{\omega - k_y V_{DeY}}{\omega_{ce}}, (k_x^2 + k_y^2) \rho^2, k_z^2 \rho^2 \right) \right]. \quad (11)$$

This result shows that contribution of EDI scales with the strength of the relative potential fluctuations ( $\phi(k_y)/T_e$ ) and the imaginary component of the Gordeev function at a particular wavevector. The imaginary component scales like the growth rate from the dispersion relation and for small  $k_z$  is significant only at the discrete gyro-resonances.<sup>18</sup> Conversely, if  $k_z$  is significant the dispersion becomes ion acoustic-like with a smoothing of the discrete resonances. In this ion acoustic limit the expression for collision frequency simplifies significantly to:<sup>19</sup>

$$\nu_{AN} \approx \sqrt{\pi} V_{the} \sum_{k_y} k_y \left( \frac{\phi(k_y)}{T_e} \right)^2 \quad (12)$$

Both Eqns.11 and 12 can be evaluated based on plume measurements. As we will describe in Section IV.B the electron temperature and axial electric field can be determined as a function of position using laser induced florescence and with a known magnetic field profile the cyclotron frequency and  $E \times B$  velocity can be inferred. The relative potential fluctuations and wavevector can be estimated using electrostatic probes. Together these measurements allows us to predict anomalous collision frequency as a function of position.

## IV. Experimental Methods

### A. Facility and Thruster

For this experiment we employed the H9, a 9-kW class Hall effect thruster developed jointly by NASA's Jet Propulsion Laboratory, the University of Michigan, and the Air Force Research Laboratory.<sup>25,26</sup> The H9 employs a magnetically shielded topography,<sup>27</sup> and uses a center-mounted LaB<sub>6</sub> hollow cathode. This thruster was tested in the Large Vacuum Test Facility (LVTF) at the University of Michigan. In this campaign, LVTF employed 10 cyropumps to reach a base pressure of  $5 \times 10^{-7}$  Torr-Xe and a working pressure of  $7 \times 10^{-6}$  Torr-Xe as recorded by a Stabil Ion gauge located approximately 1 meter adjacent to the thruster exit plane following industry standards.<sup>28</sup> The H9 was operated at 300V and 15A with a xenon flow rate of 163 scm through the anode and a 7% cathode flow fraction. The thruster body was electrically tied to the cathode.

### B. Laser Induced Florescence Measurements

Following the works Perez-Luna and Dale, the anomalous collision frequency can be determined non-invasively through laser-induced fluorescence (LIF) measurements.<sup>29,30</sup> Laser light sent into the discharge targeting the Xenon  $5d[4]_{7/2} - 6p[3]_{5/2}$  transition. The laser is detuned such that only the population of ions with a velocity that Doppler shifts the detuned wavelength into the targeted translation undergoes fluorescence. By sweeping the detuned wavelength the normalized velocity distribution function can be resolved by measuring the fluorescence intensity as a function of wavelength.

In this experiment the laser is injected axially along channel centerline and the collection optics intersects the beam at  $30^\circ$ . The beams are focused to form a  $1\text{mm}^3$  observation volume in the thruster plume. The laser wavelength is monitored using a precise wavemeter. The fluorescence is isolated from background signals through use of monochromater filtering, amplification with a photomultiplier tube and transimpedence multiplier, and homodyning with a lock-in amplifier. The measurement is repeated at points along channel centerline from the exit plane of the thruster to a little more than half a channel length downstream.

We use the VDFs to determine the plasma properties by taking the moments of the Boltzmann equation at steady state:

$$\frac{\partial \bar{u}n}{\partial z} = \dot{n}_0, \quad (13)$$

$$\frac{\partial \bar{u}^2 n}{\partial z} - \frac{e}{m} n E = 0, \quad (14)$$

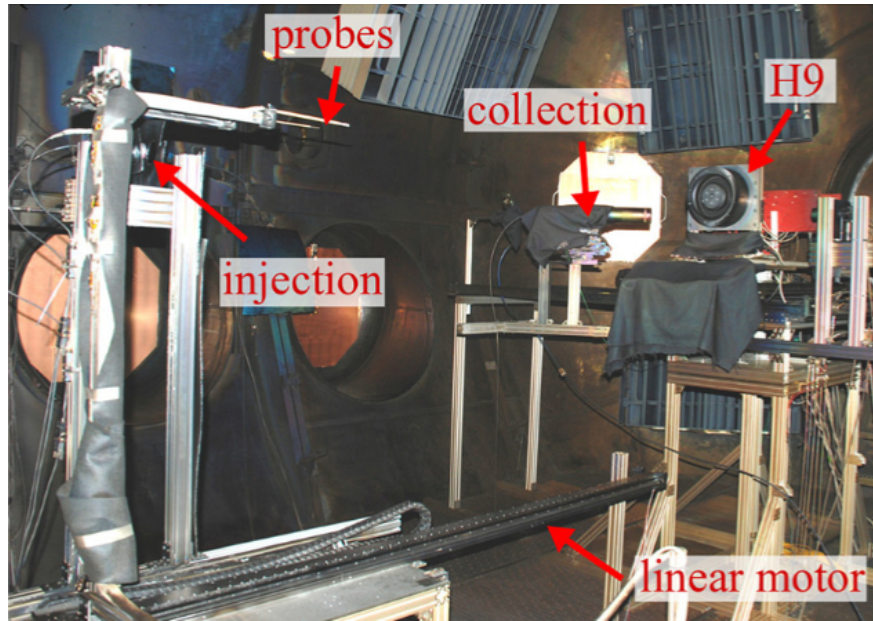


Figure 2: Experimental setup showing H9 Hall thruster, LIF optics, and high-speed injection stage.

$$\frac{\partial \bar{u}^3 n}{\partial z} - 2 \frac{e}{m} n E \bar{u} = 3 \frac{e}{m} T_i \dot{n}_0. \quad (15)$$

Here  $\bar{u}^y = \int u^y f(u) du / n$ ,  $\dot{n}_0$  is the ionization rate, and  $T_i$  is the ion temperature. These equations can be explicitly solved for  $\dot{n}_0$ ,  $E_z$ , and  $\frac{\partial n}{\partial z}$ . By using a downstream boundary condition for plasma density the gradient can be marched upstream solve for density everywhere along the measured LIF profile. The boundary condition is determined using the ion-saturation probes employed to measure wave properties (Sec IV.C). The electron temperature is calculated using empirical fitting equations for the ionization rate coefficient, the product of ionization frequency and plasma density.<sup>31</sup>

Using these parameters the total collision frequency ( $\nu_{te}$ ) can be calculated from the electron momentum equation as

$$\nu_{te} = \frac{\epsilon \pm \sqrt{\epsilon^2 - [2V_{Dex} B_r]^2}}{2 \frac{m}{e} (V_{Dex})}. \quad (16)$$

Here we maintain the electron pressure and ion resistivity terms where  $\epsilon \equiv E_x + \frac{\nabla p_e}{n_0} - \eta j_i$ . While the axial electron velocity ( $V_{Dex}$ ) cannot be directly measured we estimate it by using the discharge current density ( $j_d$ ) and ion beam velocity as ( $V_{Dex} = j_d / n_0 - V_p$ ). The anomalous collision frequency is calculated by subtracting from  $\nu_{te}$  the classical collision frequency due to electron-neutral and electron-ion collisions.

### C. Plasma Turbulence Measurements

We employed a pair of translating cylindrical Langmuir probes biased to ion saturation to characterize the plasma oscillations in the plume of the H9 thruster. The probes were made from 0.38 mm radius tungsten rods with an exposed length of 3.8 mm. In principle, the current collected on these probes should be proportional to the ion density,  $i_{sat} \propto n_i$ . In this work, we exploit this fact and follow Ref. 32 to relate measured fluctuations in the ion saturation current to plasma potential oscillations by:  $\delta i / i = \delta n / n \approx \delta \phi / T_e$ . This approximation is based on the assumption that the electron temperature and sheath dimensions do not change substantially on the time-scale of the high-speed fluctuations we are measuring. Simulations of Langmuir probes have shown that even large changes in electron temperature only marginally perturb the relationship between density and ion saturation current.<sup>33</sup> Additionally, simulations of the EDI have shown the relation  $\delta n / n \approx \delta \phi / T_e$  is generally satisfied for the EDI.<sup>9,14</sup> Finally, by performing a Fourier and Beall analysis on the probe pairs the oscillation intensity can be determined as a function of frequency and wavenumber.<sup>22,34,35</sup>

## V. Results and Discussion

The plasma parameters calculated using the Boltzmann analysis described in Section III. are plotted in Figure. 3 as function of position normalized by the thruster channel length with  $z/L = 1$  denoting the exit plane of the thruster. We indicate location of the peak magnetic field at  $z/L = 1.33$  with a dashed line. As expected for a magnetically shielded Hall thruster the acceleration region is downstream of the exit plane with the peak electric field occurring at  $z/L = 1.1$ . In this region the electron temperature peaks at 40 eV and the density is on the order of  $5e17 \text{ m}^{-3}$ . Downstream the density decays to below  $3e17 \text{ m}^{-3}$  while the electron temperature goes to about 4 eV. The anomalous collision frequency calculated using Eqn.16 is given in Figure 5. As expected the minimum collision frequency occurs at the acceleration region and increases in the near-field plume. The power spectra for select locations in the plume are shown

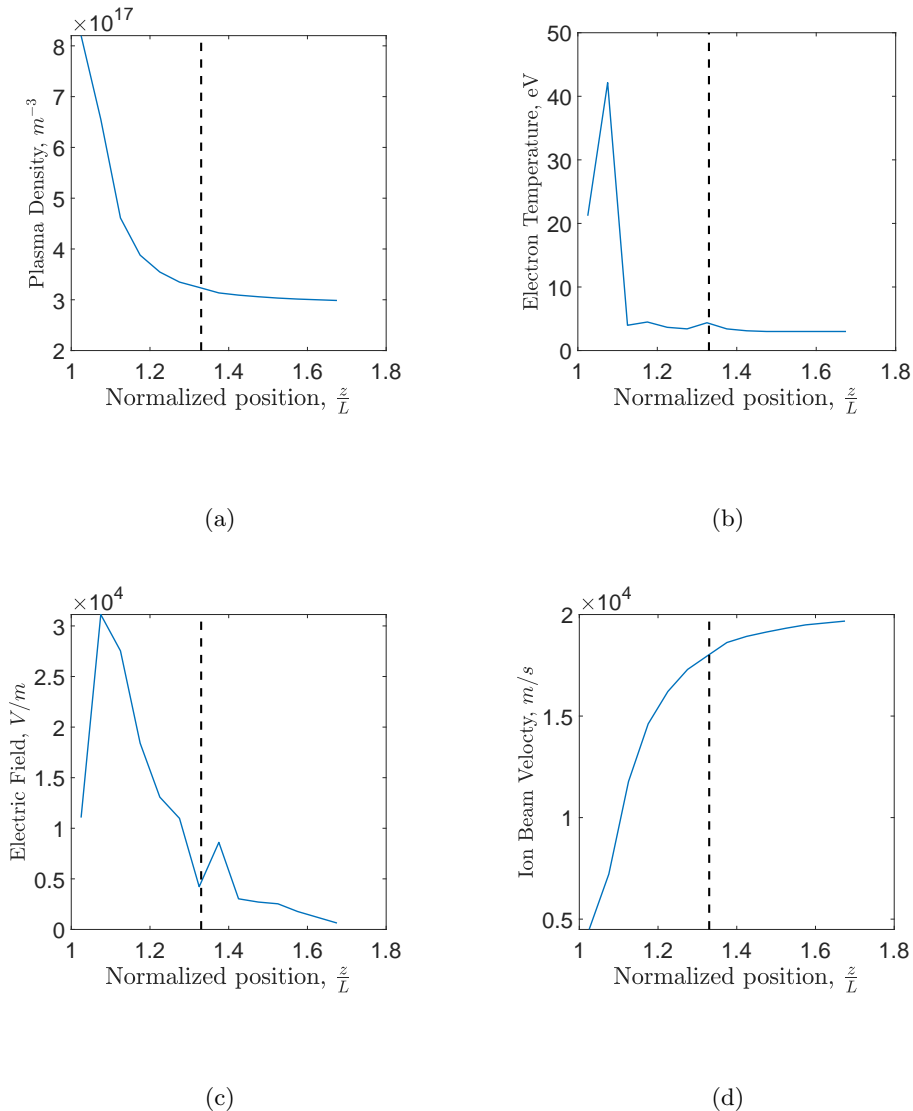


Figure 3: Plasma properties inferred from LIF measurements. Plasma density a), electron temperature b), axial electric field c), and ion beam velocity d) are plotted against axial position normalized by the channel length where  $z/L = 1$  is the exit plane of the thruster. The peak magnetic field is denoted by the dashed black line at  $z/L = 1.33$ .

in Figure. 4 and as discussed in previous studies of plasma wave turbulence there is low frequency content in the 100kHz to 1MHz range belonging to an acoustic-like wave propagating primarily in the azimuthal

direction while discrete peaks in the MHz regions are likely due to the gyro-resonances of the EDI.<sup>22,36</sup> The relative amplitude of both the acoustic and discrete waves increase as the oscillations convect downstream.

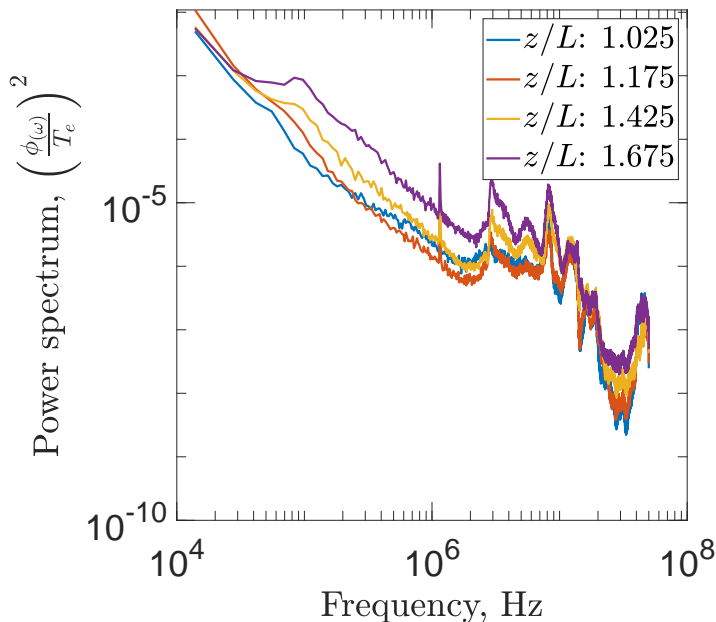


Figure 4: Power spectrum of plasma turbulence at select position in the plume.

In order to evaluate our equations for anomalous collision frequency we must make a few assumptions when converting these spectra from frequencies to wavenumbers. Since the peaks in the spectrum are rather broad there is the possibility the EDI is shifting towards the acoustic limit discussed in Section III. If this is the case we can approximate the wavenumber as scaling with the ion sound speed,  $\omega/k_y \approx C_s$ , with  $C_s = \sqrt{qT_e/M}$ . Alternatively if the modes are closer to the discrete dispersion (Eqn. 6) then consideration must be paid toward the assumptions for  $k_x$  and  $k_z$  in the Gordeev function. Previous results have shown the EDI is oriented into the plasma beam by approximately 15 degrees<sup>21,36</sup> so we assume  $k_x = k_y \sin(15^\circ)$ . We do not possess a direct measurement for  $k_z$  and its bounds are more troublesome to estimate. As has been demonstrated in numerous works, smaller  $k_z$  tends to increase the growth rate on the resonances and similarly their contribution to transport. To start we take a typical assumption that  $k_z$  is on the order of  $2\pi/\Delta R$ , where  $\Delta R$  is the channel width of the thruster. For this thruster the value of  $k_z L_{De}$  is of the order 0.01 for most of the plume. Furthermore, due to uncertain in measurements of wave turbulence the imaginary component of the Gordeev function would likely evaluate peaks at frequencies the do not perfectly match the measured resonance peaks. In general this precludes direct evaluation of the Gordeev function in our calculations. Instead we have performed an investigation of the Gordeev function for our measured plasma parameters and used the average value of the imaginary component at each predicted resonance in solving Eqn. 11. This value was typically on the order of 2 for our choice of  $k_z$ .

Subject to these assumptions the anomalous collision frequency for either a discrete or acoustic-like EDI is plotted in Figure 5. We see that due to the stronger dependence on the local plasma parameters for the discrete form of the EDI its general shape closely matches the LIF measurements. Although, it consistently under predicts the collision frequency by about a factor of 5-10. The acoustic-like solution follows a similar trend to the measured value, but under predicts the collision frequency everywhere. While the acoustic limit has few knobs available to adjust its amplitude, as discussed above the contribution of the discrete EDI heavily depends on the assumption of  $k_z$ . For example, since the acceleration region of this thruster is

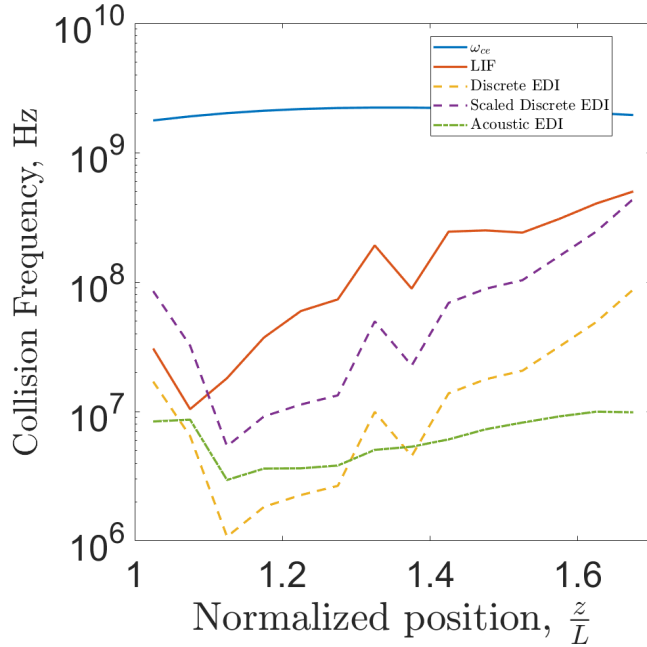


Figure 5: Anomalous collision frequency from LIF measurements and quasi-linear theory for the EDI the discrete and acoustic limit. For the discrete EDI two results for different scaling parameters of the Gordeev function are shown. The electron cyclotron frequency is also shown as a reference.

beyond the channel walls the radial wavenumber may be even lower than  $2\pi/\Delta R$ . If we lower the  $k_z L_{De}$  by a factor of ten the average value of the imaginary component of the Gordeev function at the resonances raises to 10-15. When using this scaling coefficient the discrete EDI results in the anomalous collision frequency seen in Figure. 5 denoted as “Scaled Discrete EDI”. This profile agrees with the measured collision frequency to within a factor of 3 for most the plume, but now overestimates in the acceleration zone by a factor 5.

For the discrete EDI there seems to be decent agreement between theory and measurement throughout the plume, and both limits of the EDI match well in the acceleration region. Although it is peculiar that our theory for the EDI does not consistently over or under predict the anomalous collision frequency. For the discrete EDI when assume  $k_z$  is very small, in the near-field plume the theory slightly under predicts the collision frequency, yet it over predicts in the acceleration zone. This may be indicative of higher order effects in the instability not captured by the quasilinear theory presented in Sections II and III. In particular we have assumed the electron velocity distribution function is Maxwellian, but several PIC codes have resolved non-Maxwellian distributions which significantly affect how the EDI contributes to transport. In the acoustic-limit, non-Maxwellian distributions lower the anomalous resistivity due to the EDI, potentially by a factor of 2-5.<sup>37</sup> For the discrete EDI the situation is more nebulous as Ducrocq showed that depending on which resonance number is being considered non-Maxwellian electrons can either increase or decrease the instability growth rate by a factor of 2-4, but with a tendency towards reduction.<sup>17</sup> We plot the ratio of the scaled discrete EDI and acoustic EDI to the measured collision frequency (Fig. 6) and observe that the ratio in the acceleration zone is on the order expected from non-Maxwellian effects for discrete limit. Perhaps in this region where the  $E \times B$  drift velocity is largest and the instability develops the electrons distribution becomes distorted reducing the impact of the instability. Further downstream the electrons may thermalize allowing the instability to contribute more to cross-field transport. We also note that the differences in the scaling parameter could be due to changes in the dispersion relation as the instability develops and propagates in the plume. Recent simulations have shown that the EDI can undergo significant nonlinear changes and an inverse energy cascade towards long wavelength as it propagates.<sup>10,11</sup> Similarly, the Cartesian approximation used in the formulation of the EDI dispersion may not be appropriate for the long wavelength content measured and an analysis in cylindrical coordinates is more prudent. It is also possible that our electrostatic wave probes disturb the instability in some way.

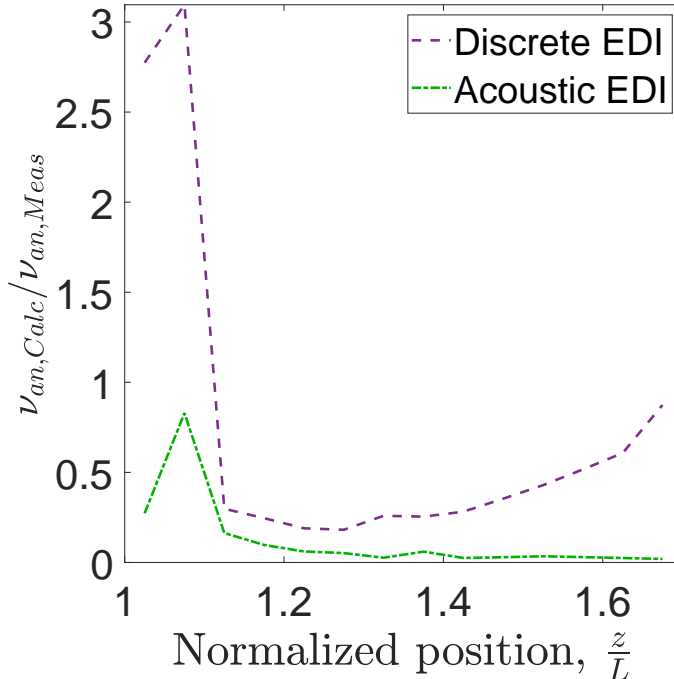


Figure 6: Ratio of the predicted anomalous collision frequency to LIF inferred measurements as a function of position in the plume.

## VI. Conclusion

In this paper we have presented the results of an investigation on anomalous electron transport in a Hall thruster plume. We implemented a measurement diagnostic capable of directly measuring the anomalous collision frequency and plasma wave turbulence that we use to predict the collision frequency from quasi-linear theory of the electron drift instability. The measured anomalous collision frequency is at a minimum in the narrow acceleration zone just past the exit plane of thruster and increases further downstream. The plasma turbulence is characterized by both high frequency resonances and low frequency acoustic-like oscillations. When applying quasi-linear theory for the electron drift instability we predicted an anomalous collision frequency on the order of the measured values. Although there were notable discrepancies, particularly in the acceleration zone, where the EDI theory overestimates the collision frequency by a factor of 5 for the discrete EDI while the acoustic theory under predicts everywhere in the plume. We discussed that in the context of recent numerical work this may be indicative on non-Maxwellian electrons in the acceleration zone or other non-linear effects. Together these results give further confidence that the EDI plays a dominant role in electron cross field transport and highlight the necessity of advancing the theoretical models for predicting anomalous transport and eventual incorporation into a closure equation for hybrid-based codes.

## Acknowledgments

Work supported by National Science Foundation Graduate Research Fellowship Program Grant No DGE 1256260. Any opinions, findings, and conclusions or recommendations expressed in this material are those of the author(s) and do not necessarily reflect the views of the National Science Foundation.

## References

- <sup>1</sup>Choueiri, E. Y., “Plasma oscillations in Hall thrusters,” *Physics of Plasmas*, Vol. 8, 2001, pp. 1411.
- <sup>2</sup>Boeuf, J. P., “Tutorial: Physics and modeling of Hall thrusters,” *Physics of Plasmas*, Vol. 121, No. 1, 2017, pp. 011101.

- <sup>3</sup>Meezan, N. B., Hargus, W. A., and Cappelli, M. A., “Anomalous electron mobility in a coaxial Hall discharge plasma,” *Physics Review E*, Vol. 62, No. 2, 2001, pp. 026410.
- <sup>4</sup>Boniface, C., Garrigues, L., Hagelaar, G. J. M., Boeuf, J. P., Gawron, D., and Mazouffre, S., “Anomalous cross field electron transport in a Hall effect thruster,” *Applied Physics Letters*, Vol. 89, No. 16, 2006, pp. 161503.
- <sup>5</sup>Barral, S., Makowski, K., Peradzyski, Z., Gascon, N., and Dudeck, M., “Wall material effects in stationary plasma thrusters. II. Near-wall and in-wall conductivity,” *Physics of Plasmas*, Vol. 10, No. 10, 2003, pp. 4137.
- <sup>6</sup>Gascon, N., Dudeck, M., and Barral, S., “Wall material effects in stationary plasma thrusters. I. Parametric studies of an SPT-100,” *Physics of Plasmas*, Vol. 10, No. 10, 2003, pp. 4123.
- <sup>7</sup>McDonald, M. S. and Gallimore, A. D., “Parametric Investigation of the Rotating Spoke Instability in Hall Thrusters,” *32nd International Electric Propulsion Conference*, 2011.
- <sup>8</sup>Ellison, C. L., Raitses, Y., and Fisch, N. J., “Cross-field electron transport induced by a rotating spoke in a cylindrical Hall thruster,” *Physics of Plasmas*, Vol. 11, No. 1, 2012, pp. 013503.
- <sup>9</sup>Laffeur, T., Baalrud, S. D., and Chabert, P., “Theory for the anomalous electron transport in Hall effect thrusters: I. Insights from particle-in-cell simulations,” *Physics of Plasmas*, Vol. 23, 2016, pp. 053502.
- <sup>10</sup>Janhunen, S., Smolyakov, A., Chapurin, O., Sydorenko, D., Kaganovich, I., and Raitses, Y., “Nonlinear structures and anomalous transport in partially magnetized EB plasmas,” *Physics of Plasmas*, Vol. 25, No. 1, 2018, pp. 011608.
- <sup>11</sup>Janhunen, S., Sydorenko, A., Sydorenko, D., Jimenez, M., Kaganovich, I., and Raitses, Y., “Evolution of the electron cyclotron drift instability in two-dimensions,” *Physics of Plasmas*, Vol. 25, No. 8, 2018, pp. 082308.
- <sup>12</sup>Ortega, A. L., Katz, I., and Chaplin, V. H., “A First-Principles Model Based on Saturation of the Electron Cyclotron Drift Instability for Electron Transport in Hydrodynamic Simulations of Hall Thruster Plasmas,” *35th International Electric Propulsion Conference*, 2017.
- <sup>13</sup>Boeuf, J. P. and Garrigues, L., “E x B electron drift instability in Hall thrusters: Particle-in-cell simulations vs. theory,” *Physics of Plasmas*, Vol. 25, 2018, pp. 061204.
- <sup>14</sup>Hron, A. and Adam, J. C., “Anomalous conductivity in Hall thrusters: Effects of the non-linear coupling of the electron-cyclotron drift instability with secondary electron emission of the walls,” *Physics of Plasmas*, Vol. 20, No. 8, 2013, pp. 082313.
- <sup>15</sup>Katz, I., Chaplin, V. H., and Ortega, A. L., “Numerical Studies of Hall Thruster Acceleration Region Electron Transport,” *2018 Joint Propulsion Conference, AIAA Propulsion and Energy Forum*, 2018.
- <sup>16</sup>Boeuf, J. P. and Smolyakov, A., “Preface to Special Topic: Modern issues and applications of EB plasmas,” *Physics of Plasmas*, Vol. 25, No. 6, 2018, pp. 061001.
- <sup>17</sup>Ducrocq, A., Adam, J. C., and Heron, A., “High-frequency electron drift instability in the cross-field configuration of Hall thrusters,” *Physics of Plasmas*, Vol. 13, No. 10, 2006.
- <sup>18</sup>Cavaliere, J., Lemoine, N. and Bonhomme, G., Tsikata, S., Honore, C., and Gresillon, D., “Hall Thruster Plasma Fluctuations Identified as the ExB Electron Drift Instability: Modeling and Fitting on Experimental Data,” *Physics of Plasmas*, Vol. 20, 2013, pp. 082108.
- <sup>19</sup>Laffeur, T., Baalrud, S. D., and Chabert, P., “Theory for the anomalous electron transport in Hall effect thrusters: II. Kinetic model,” *Physics of Plasmas*, Vol. 23, 2016, pp. 053503.
- <sup>20</sup>Tsikata, S., Lemoine, N., Pisarev, V., and Gresillon, D. M., “Dispersion relation of electron density fluctuations in a Hall thruster plasma, observed by collective light scattering,” *Physics of Plasmas*, Vol. 16, No. 3, 2009, pp. 033506.
- <sup>21</sup>Tsikata, S., Honore, C., Lemoine, N., and Gresillon, D. M., “Three-dimensional structure of electron density fluctuations in the Hall thruster plasma: E x B mode,” *Physics of Plasmas*, Vol. 17, No. 11, 2010, pp. 112110.
- <sup>22</sup>Brown, Z. A. and Jorns, B. A., “Dispersion relation measurements of plasma modes in the near-field plume of a 9-kW magnetically shielded thruster,” *35th International Electric Propulsion Conference*, 2017.
- <sup>23</sup>Davidson, R. and Krall, N., “Anomalous transport in high-temperature plasmas with applications to solenoidal fusion systems,” *Nuclear Fusion*, Vol. 17, 2018, pp. 1313.
- <sup>24</sup>Adam, J. C., Heron, A., and Laval, G., “Study of stationary plasma thrusters using two-dimensional fully kinetic simulations,” *Physics of Plasmas*, Vol. 11, No. 1, 2004, pp. 295.
- <sup>25</sup>Hofer, R. R., Cusson, S. E., and Lobbia, R. B., “The H9 Magnetically Shielded Hall Thruster,” *35th International Electric Propulsion Conference*, 2017.
- <sup>26</sup>Cusson, S. E., Hofer, R. R., Lobbia, R. B., Jorns, B. A., and Gallimore, A., “Performance of the H9 Magnetically Shielded Hall Thrusters,” *35th International Electric Propulsion Conference*, 2017.
- <sup>27</sup>Mikellides, I. G., Katz, I., Hofer, R., and Goebel, D., “Magnetic shielding of walls from the unmagnetized ion beam in a Hall thruster,” *Applied Physics Letters*, Vol. 102, No. 2, 2013, pp. 023509.
- <sup>28</sup>Dankanich, J. W., Walker, M., Swiatek, M. W., and Yim, J. T., “Recommended Practice for Pressure Measurement and Calculation of Effective Pumping Speed in Electric Propulsion Testing,” *Journal of Propulsion and Power*, Vol. 33, No. 3, 2017, pp. 668–680.
- <sup>29</sup>Pérez-Luna, J., Hagelaar, G. J. M., Garrigues, L., and Boeuf, J. P., “Method to obtain the electric field and the ionization frequency from laser induced fluorescence measurements,” *Plasma Sources Science and Technology*, Vol. 18, No. 3, jul 2009, pp. 034008.
- <sup>30</sup>Dale, E. T. and Jorns, B. A., “Non-invasive time-resolved measurements of anomalous collision frequency in a Hall thruster,” *Physics of Plasmas*, Vol. 26, No. 1, 2019, pp. 013516.
- <sup>31</sup>Goebel, D. and Katz, I., *Fundamentals of Electric Propulsion: Ion and Hall Thrusters*, John Wiley and Sons, 2008.
- <sup>32</sup>Jorns, B. A., Mikellides, I. G., and Goebel, D. M., “Ion acoustic turbulence in a 100-A LaB<sub>6</sub> hollow cathode,” *Phys. Rev. E*, Vol. 90, Dec 2014, pp. 063106.
- <sup>33</sup>Nold, B., Ribeiro, T. T., Ramisch, Huang, Z., Müller, H. W., Scott, B. D., and Stroth, U., “Influence of temperature fluctuations on plasma turbulence investigations with Langmuir probes,” *New Journal of Physics*, Vol. 14, 2012, pp. 063022.
- <sup>34</sup>Jorns, B. and Hofer, R., “Plasma oscillations in a 6-kW magnetically shielded Hall thruster,” *Physics of Plasmas*, Vol. 21, No. 5, 2014, pp. 053512.

- <sup>35</sup>Beall, J. M., Kim, Y. C., and Powers, E. J., "Estimation of wavenumber and frequency spectra using fixed probe pairs," *Physics of Plasmas*, Vol. 53, 1982, pp. 3933.
- <sup>36</sup>Brown, Z. and Jorns, B. A., *Spatial Evolution of Plasma Waves in the Near-field of a Magnetically Shielded Hall Thruster*.
- <sup>37</sup>Laffeur, T., Chabert, P., and Bourdon, A., "Anomalous electron transport in Hall-effect thrusters: Comparison between quasilinear kinetic theory and particle-in-cell simulations," *Physics of Plasmas*, Vol. 25, 2018, pp. 061202.